International Journal of Scientific Research in Engineering and Management (IJSREM)
Volume: 10 Issue: 03 | March - 2026 SJIF Rating: 8.659 ISSN: 2582-3930

Design and Fabrication of the Underwater Robot

B. Gowtham[1], L.G. Bharanidharan[2], K.B. Pragadeshwaran[3], N. Vasudevan[4]

[1,2,3]Undergraduate Student, Department of Mechanical Engineering, Sri Sai Ram Engineering College
[4]Associate Professor, Department of Mechanical Engineering, Sri Sai Ram Engineering College

---

Abstract

Corrosion continues to be a critical concern for submerged metallic structures such as ship hulls, offshore platforms, and marine pipelines, especially due to the harsh marine environment. Conventional inspection methods relying on human divers often involve high cost, extended time, and considerable risk. This paper discusses the design and theoretical analysis of a Remotely Operated Vehicle (ROV) prototype developed for the purpose of non-destructive inspection. The system incorporates a modular stainless-steel frame for stability, supported by bilge-pump based propulsion that enable precise maneuverability. A structured framework including buoyancy estimation, thrust force calculation, and structural validation was established to ensure operational reliability. The prototype was tested in a controlled aquatic setup, confirming stable locomotion and effective control, thereby demonstrating readiness for integration with corrosion detection modules. This framework highlights the feasibility of employing an ROV as a cost-effective, safe, and reliable platform for real-time underwater structural health monitoring.

Keywords: Corrosion, Remotely Operated Vehicle, Non-Destructive Inspection, Bilge Pump, Propulsion, Locomotion.

1. Introduction

Corrosion of submerged metallic structures remains a critical challenge in industries such as shipbuilding, offshore platforms, and pipelines, where continuous seawater exposure accelerates material degradation. Conventional inspection methods carried out by divers are hazardous, time-consuming, and costly, with limited efficiency in prolonged operations. This paper discusses the design and development of a Remotely Operated Vehicle (ROV) prototype intended as a dedicated platform for underwater non-destructive testing. The system employs a modular stainless-steel frame engineered for robustness, coupled with a custom bilge-pump-based propulsion system to ensure maneuverability and stability.

A structured framework including material selection, buoyancy estimation, stability analysis, and thrust calculations is presented to validate the design. The prototype was fabricated and tested in a controlled aquatic environment, demonstrating stable locomotion, precise control, and reliability. This framework establishes the viability of employing the ROV as a cost-effective, safe, and adaptable mobile platform, enabling future integration of corrosion detection sensors for real-time underwater structural health monitoring.

2. Fundamentals of Underwater Robot Design

The design of ROV is based on fundamental principles of hydrostatics, hydrodynamics, and power-control systems. A proper understanding of these ensures the ROV is stable, maneuverable, and efficient in underwater operations.

Hydrostatics: Buoyancy and Stability

The static equilibrium of the ROV is determined by the balance of weight and buoyant force.

Archimedes' Principle - The buoyant force acting on a submerged body is given by: $F_b = \rho . g . V$

Where, F_b = buoyant force (N),
ρ = Density of fluid (kg/m^3);
g = Acceleration due to gravity (9.81 m/s^2);
V= Volume of displaced fluid (m^3)

Buoyancy States - 1. Positively Buoyant: $F_b > W \rightarrow$ Vehicle floats.
2. Negatively Buoyant: $F_b < W \rightarrow$ Vehicle sinks.
3. Neutrally Buoyant: $F_b = W \rightarrow$ Vehicle hovers.

Static Stability - Center of Buoyancy (C_B): Centroid of displaced water. Center of Gravity (C_G): Centroid of mass of the vehicle. For stability: C_G must be vertically above CG, generating a righting moment against tilting.

Hydrodynamics: Drag and Thruster Configuration

The movement of an ROV underwater is affected by drag forces and thrust forces. Drag Force - For low-speed ROVs:

$F_d = (0.5) \cdot C_d \cdot \rho \cdot A \cdot v^2$

Where, F_d = Drag force (N)
C_d = Drag coefficient (depends on shape)
ρ = Fluid density (kg/m³)
A = Projected area of body (m²)
v = Velocity of ROV (m/s)

Types of Drag – Pressure Drag: Due to pressure difference across the body. Skin Friction Drag: Due to viscosity and surface roughness.

Thruster Configuration & Degrees of Freedom –

ROVs operate in 6 DOF: Surge, Sway, Heave, Roll, Pitch, Yaw. In this design, 3 thrusters provide 3 DOF control.

Two Horizontal Thrusters → Surge (forward/backward) + Yaw (rotation). One Vertical Thrusters → Heave (up/down).

Power and Control Systems

Power Supply- Delivered via tether from surface 12V onboard for thrusters & electronics.

Control Architecture - Surface Control Unit → PC interface.
Onboard Microcontroller (Arduino UNO) → Receives commands, processes control logic. Motor Drivers / ESCs → Convert signals into high-power PWM for thrusters.

3. Literature Survey

The evolution of underwater robotic platforms has been driven by the need to replace hazardous and costly human diver operations with reliable, untethered, or lightly tethered systems capable of executing complex inspection tasks. The foundational challenges in this domain were systematically outlined by Yuh [1], who provided a comprehensive survey of autonomous underwater vehicle (AUV) design and control.

This seminal work identified that the primary technical hurdles including the management of nonlinear hydrodynamics, the variability of added mass, and the need for robust, fault-tolerant control systems - stem from the unstructured and unpredictable nature of the underwater environment. Yuh established that a successful vehicle design must integrate adaptive control strategies to handle parameter uncertainties and sensor noise, laying the groundwork for all subsequent developments in intelligent underwater robotics. Building on this, Whitcomb [2] chronicled the transition of underwater robotics from laboratory curiosities to indispensable tools for deep-water scientific and commercial applications. His review highlighted critical advancements in high-power-density propulsion, efficient power distribution systems, and reliable through-water telemetry, which collectively enabled the development of vehicle classes specifically tailored for tasks such as pipeline inspection, cable burial, and deep-sea exploration.

The practical challenges of implementing stable and controllable Remotely Operated Vehicles (ROVs) were rigorously investigated by Azis et al. [3] through a detailed case study. Their work dissected the complexities of depth control and station-keeping, identifying that these functions are often compromised by underactuated configurations, coupling between degrees of freedom, and communication latency inherent in tethered systems.

The study concluded that robust performance in hazardous environments necessitates an interdisciplinary approach that combines advanced control theory with a deep understanding of the vehicle's hydrodynamic profile. This practical perspective was complemented by the work of Chevallareau et al. [4], who introduced a bio-inspired approach to coordinated underwater navigation. By employing a follower-leader multi-agent strategy combined with direct servo control of electric sense measurements, their research demonstrated how biologically plausible control laws can achieve precise navigation and formation keeping. The convergence properties of their control law were rigorously proven, offering a sophisticated alternative to traditional, model-based approaches and opening new possibilities for cooperative inspection tasks.

The pursuit of low-cost, accessible platforms has been a parallel and equally important stream of research, particularly for educational and preliminary proof-of-concept work. El-Fakdi and Cufí [5] presented a long-term initiative aimed at engaging secondary school students by having them construct underwater robotic vehicles using low-cost, readily available materials. Over a 13-year period, this project involved over 800 students in the fabrication of approximately 200 vehicles,

demonstrating that sophisticated concepts like AUV navigation could be implemented using open-source platforms like Arduino. A critical practical contribution of this work was the development of motor encapsulation techniques, which enabled the safe and reliable use of standard 12V DC motors in a submerged environment.

This approach directly validates the use of cost-effective components, such as bilge pumps, for proof-of-concept ROVs. Nita et al. [6] detailed a complete system architecture for a remotely controlled underwater robot, comprising a surface control interface, an intermediate device, and the robot itself. Their system, equipped with eight electric motors for full six-degree-of-freedom (6-DOF) control and two video cameras, illustrated the complexity required for versatile navigation and surveillance, while also highlighting the limitations imposed by the umbilical tether, which is often managed with a Tether Management System (TMS) for deep-water operations.

Recent advancements have focused on enhancing the intelligence and navigational autonomy of these platforms. Hung and Na [7] developed a sophisticated remote-control system for a 6-DOF underwater robot, demonstrating precise joystick-based control facilitated by robust onboard processing. Szymak [8] explored the cutting edge of biomimetic design, investigating underwater vehicles that emulate the locomotion of fish and other marine creatures. This research into biologically inspired propulsion and maneuvering promises significant improvements in efficiency and agility compared to traditional propeller-driven craft, particularly in complex, cluttered environments.

The challenge of multi-robot coordination was addressed by Joordens and Jamshidi [9], who applied consensus control algorithms to a system of underwater swarm robots. Their work demonstrated that through localized communication and decentralized control, a swarm of simple robots could achieve coordinated behaviors, such as collective exploration or formation movement, offering a scalable and robust alternative to single, complex, and expensive vehicles.

The integration of advanced manipulation and sensing capabilities has further expanded the utility of underwater robots. Mazzeo et al. [10] provided a comprehensive taxonomy of underwater manipulative actions required for deep-sea specimen collection, categorizing the functional requirements for robotic arms and grippers in scientific sampling tasks. Wang et al. [11] described the design and development of an intelligent underwater robot capable of autonomous decision-making based on sensor inputs, moving beyond simple remote control to proactive mission execution.

Finally, Potokar et al. [12] introduced HoloOcean, a high-fidelity underwater robotics simulator that provides researchers with a powerful tool for developing and testing navigation, control, and perception algorithms in realistic, repeatable environments without the cost and complexity of physical water trials. This simulator-based approach is accelerating the development cycle and enabling rapid prototyping of new capabilities for underwater inspection platforms, from corrosion detection to ecosystem monitoring.

4. Flow of Study

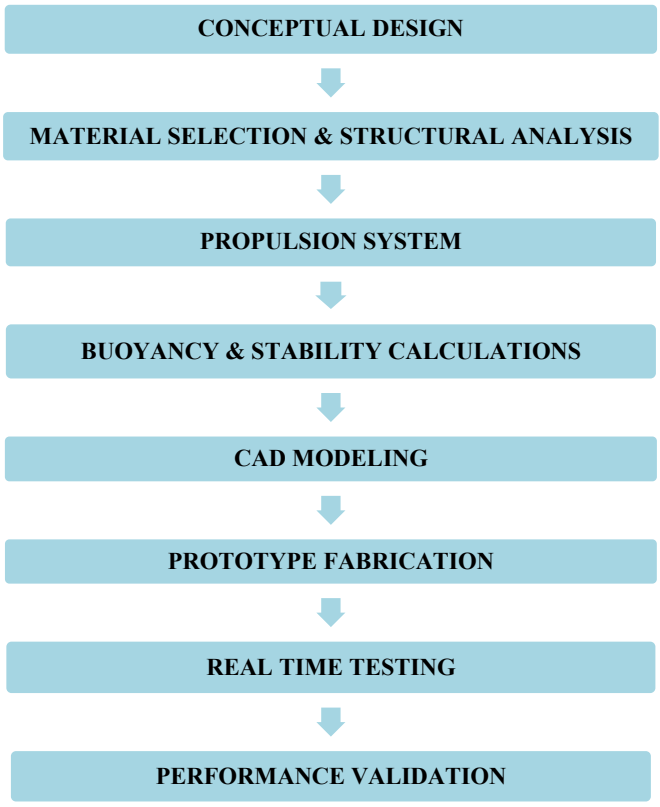

Fig 1. This flowchart presents the systematic engineering approach followed in developing the Remotely Operated Underwater Vehicle (ROV). The process initiates with the conceptual design phase and advances through key stages such as material selection, propulsion system analysis, and hydrostatic stability evaluation. Insights from these analyses guide the creation of detailed CAD models, which serve as the blueprint for prototype fabrication. The methodology concludes with controlled pool testing and performance validation, ensuring the ROV's reliability and readiness for real-world underwater inspection operations.

5. List of Components

Table 1. This Table presents a detailed breakdown of all essential components used in constructing the Remotely Operated Underwater Vehicle (ROV) prototype. It includes items from each major subsystem such as structural framework, propulsion units, control electronics, power modules, and auxiliary components along with their specifications and quantities. Together, these elements form the complete assembly required to realize the fully functional underwater robotic system.

S.NO	COMPONENT NAME	QUANTITY
1.	PVC Pipe (OD – 1.25 inch, ID – 1 inch)	4 meters
2.	Bilge Pump – 12V, 1100 GPH	3
3.	L298N Motor Driver Module	2
4.	Arduino UNO Microcontroller	1
5.	DPDT Switch	3
6.	Lead Acid Battery – 12V, 7Ah	1
7.	Tethering Cable – Multi Conductor	1
8.	Propeller Blades	3
9.	Polyethylene Buoyancy Foam	As Required
10.	Waterproof Enclosure & Adhesives	As Required

PVC Pipe

Polyvinyl Chloride (PVC) pipes constitute the primary structural framework of this underwater robot prototype. Outer Diameter – 1.25 inch, Inner Diameter – 1 inch and Total length – 4 meters. Selected for their inherent corrosion resistance, low density, and high strength-to-weight ratio, these pipes provide a robust yet lightweight skeleton. The material's non-reactive nature in freshwater environments ensures long-term structural integrity, while its ease of fabrication allowing simple cutting, rapid prototype assembly and modification. The open-frame design minimizes hydrodynamic drag and allows for straightforward component mounting and maintenance.

Bilge Pump

The vehicle's propulsion is powered by high-efficiency, commercially available bilge pumps, 1100 GPH, which are converted to function as thrusters. Each unit is a self-contained propulsion module, featuring a sealed DC motor and an integrated impeller enclosed within a durable plastic housing. When energized by a 12V DC supply, the impeller's rotation moves water axially through the pump, generating thrust. This solution provides a cost-effective, reliable, and pre-waterproofed propulsion system, ideal for proof-of-concept vehicles and low-to-moderate speed underwater mobility.

L298N Motor Driver Module

The L298N motor driver module acts as a critical interface between the low-power control signals from the microcontroller and the high-current demands of the bilge pump motors. This dual H-bridge driver receives Pulse Width Modulation (PWM) signals from the Arduino and amplifies them to deliver the necessary voltage and current to the motors. Its capability to control the direction and speed of two DC motors independently enables precise maneuverability, including differential thrust for turning and variable speed control for forward and reverse motion.

Fig 2 & 3. These Figures gives the pictorial of Bilge Pump which functions as the vehicle's thruster, generating propulsive force. The L298N Motor Driver module acts as the intermediary power amplifier, translating PWM commands from the central microcontroller into the necessary power output to drive the pumps, thus facilitating controlled underwater maneuverability.

Arduino UNO Microcontroller

An Arduino UNO microcontroller serves as the central nervous system of the robotic platform executes the programmed control logic; processing user commands received via the tether. The Arduino generates precise PWM signals to regulate the rotational speed of each bilge pump motor, thereby controlling the thrust output. Its role is to synchronize the operation of multiple thrusters to execute complex locomotion commands such as forward movement, rotation, and vertical ascent/descent.

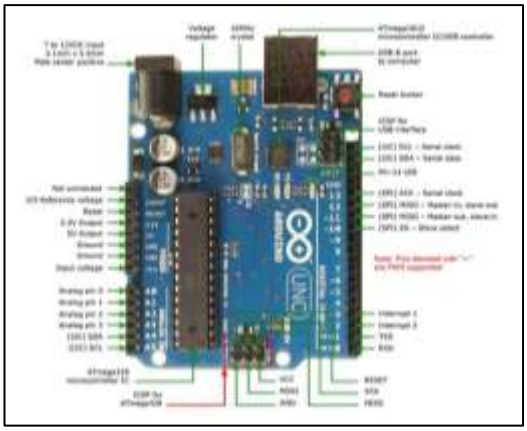

Fig 4. This Figure shows the Arduino UNO microcontroller, which acts as the primary processing core of the control subsystem of the underwater robot. It is programmed to manage the differential speed and direction of the three bilge pump thrusters, facilitating maneuvers such as forward/backward motion, yaw rotation, and vertical heave.

DPDT Switch

Double Pole Double Throw (DPDT) switches are incorporated to manually control the directional rotation of each bilge pump motor. These switches function by reversing the polarity of the voltage supplied to the motor terminals. In one position, the motor rotates forward, and in the other, the polarity is reversed, causing the motor to rotate in the opposite direction. This provides a simple, robust, and intuitive method for achieving bidirectional thrust without relying on complex electronic reversing circuits, ensuring reliable forward and backward propulsion.

Lead Acid Battery – 12V, 7Ah

A 12V, 7Ah sealed lead-acid battery provides a dependable and portable power source for the entire system. Chosen for its ability to deliver high surge currents, it meets the startup and operational demands of the bilge pump motors. The battery supplies stable power to the thrusters, motor drivers, and the Arduino controller, ensuring consistent performance during extended underwater missions. Its rechargeable nature makes it cost-effective for repeated testing and development cycles.

Fig 5 & 6. These Figures shows the DPDT (Double Pole Double Throw) switch used for manual reversal of motor polarity to achieve bidirectional thrust. And 12V, 7Ah sealed lead-acid battery that serves as the primary, high-current power source for the entire ROV system, ensuring reliable operation during submerged missions.

Tethering Cable – Multi Conductor

A multi-conductor tethering cable establishes a vital physical and electrical link between the robot and the surface control station. This cable serves a dual purpose: it ensures a continuous and stable supply of electrical power from the lead-acid battery to the onboard systems, and it transmits real-time control signals from the operator to the Arduino microcontroller. The tether guarantees uninterrupted operation and eliminates the constraints of a limited onboard battery capacity during prolonged testing sessions.

Propeller Blades

Each bilge pump is equipped with an integral propeller, a key component that converts the motor's rotational kinetic energy into linear thrust. The propeller's carefully designed blades and 3D printed accelerate a mass of water rearward, this action produces an equal and opposite force that propels the vehicle forward. The design and pitch of these blades are optimized for the specific flow characteristics of the bilge pump housing, directly influencing the system's thrust efficiency and overall hydrodynamic performance.

Polyethylene Buoyancy Foam

Closed-cell polyethylene foam is strategically attached to the robot's frame to manage its buoyancy and stability

underwater. This material is impervious to water absorption and provides significant positive buoyancy. By carefully calculating and adding the required volume of foam, the overall density of the vehicle is adjusted to achieve a near-neutrally buoyant state. This is critical for reducing the power required to maintain depth, improving stability, and ensuring the vehicle is not overly heavy or floaty during operation.

Waterproof Enclosure & Adhesives

A waterproof enclosure, typically fabricated from PVC or acrylic, is essential for housing and protecting sensitive electronics like the Arduino and motor drivers from water ingress and potential short circuits. This enclosure is sealed with gaskets and waterproof adhesives to create a dry, secure environment. PVC solvent cement and other specialized marine-grade sealants are used to permanently bond the structural frame and ensure all potential leak paths are effectively sealed, guaranteeing the operational integrity of the robot in submerged conditions.

6. Methodology

The development of the Remotely Operated Vehicle (ROV) prototype was guided by a structured engineering methodology, segmented into four core, interdependent phases. This approach ensured that the final design was not only functional but also optimized for stability, maneuverability, and cost-effectiveness, serving as a reliable platform or future sensor integration.

1. Mechanical Design and Material Selection

The primary objective of the mechanical design was to create a stable, and hydrodynamically efficient platform. The process began with a conceptual design phase where a modular, open-frame structure was selected. This architecture offers significant advantages, including ease of assembly and maintenance, reduced hydrodynamic drag, and flexibility for future modifications and component additions.

(I) Aluminum 6061: Identified as the optimal material for a commercial-grade system. It offers a superior strength-to-weight ratio, excellent durability, and good corrosion resistance when anodized. However, its higher cost and requirement for advanced fabrication techniques – welding made it less suitable for this concept prototype

(II) Polyvinyl Chloride (PVC): Selected for the prototype. Its key advantages include exceptional corrosion resistance in freshwater environments, very low density contributing to a favorable buoyancy profile, high strength-to-weight ratio for a polymer, and excellent fabricability using simple tools and solvent welding. These properties make it ideal for rapid prototyping and testing in controlled aquatic conditions. The final frame was designed using PVC pipes (OD: 1.25 inch, ID: 1 inch) assembled into a rectangular structure, providing a stable base with defined mounting points for all subsystems.

2. Propulsion System and Thruster Configuration

The propulsion system was designed to generate sufficient thrust for controlled maneuverability while overcoming hydrodynamic drag. The selection process prioritized reliability, cost, and simplicity. Thruster Selection: Commercially available 12V DC bilge pump, 1100 GPH flow rate were chosen as thrusters.

This selection was strategic, as their pre-sealed, waterproof housings eliminated the need for complex and custom waterproofing of motors. Each pump functions as a self-contained axial-flow thruster, where an integrated impeller accelerates water to produce thrust.

Thruster Configuration for 3-DOF Control: A three-thruster configuration was implemented to provide control in three critical degrees of freedom (DOF), balancing simplicity with functional capability: Two Horizontal Thrusters: Mounted parallel to the longitudinal axis on opposite sides of the frame. Operated in unison, they provide surge - forward/backward motion. Operated differentially one forward, one backward or at different speeds, they generate a torque for yaw - left/right rotation.

One Vertical Thruster: Mounted centrally to provide heave - up/down motion, allowing the vehicle to change depth and maintain altitude. This configuration provides effective and intuitive control for basic inspection maneuvers.

3. Buoyancy and Hydrostatic Stability Analysis

Achieving stable and efficient underwater operation was paramount. This phase involved precise calculations and a systematic approach to ensure the vehicle could maintain depth and orientation with minimal power expenditure. The primary objective was to achieve a near-neutrally buoyant state. A perfectly neutrally buoyant vehicle hovers effortlessly, while a slightly positive one floats to the surface if power is lost—a critical safety feature. The process was as follows:

Weight Estimation (W): The total weight of the complete vehicle was meticulously calculated by summing the masses of all components:

i. Structural Frame (PVC pipes and fittings)
ii. Propulsion System (3 bilge pumps)
iii. Electronics (Camera Module, Tethering Cable)

This total mass (m_{total}) was converted to weight: $\mathbf{W = m_{total} * g}$, where g is the acceleration due to gravity (9.81 m/s^2).

Displacement Volume (V) and Buoyant Force (F_b): The total volume of water displaced by the submerged structure and components was estimated. For the PVC frame, this was calculated based on the external dimensions of the pipes. The theoretical buoyant force was then determined using Archimedes' principle**:**

$$\mathbf{F_b = \rho_{water} * g * V}$$

where, ρ_{water} is the density of freshwater (1000 kg/m^3).

Buoyancy Deficit/Surplus Analysis: The initial buoyant force (F_b) was compared to the vehicle's weight (W):

i. If $W > F_b$, the vehicle is negatively buoyant and will sink.
ii. If $W < F_b$, the vehicle is positively buoyant and will float.

Buoyancy Compensation: To achieve near-neutral buoyancy, the deficit or surplus had to be corrected. Closed-cell polyethylene foam was chosen as the buoyancy aid due to its negligible water absorption and high positive buoyancy. The required volume of foam (V_{foam}) was calculated using - **Buoyancy Deficit = W - F_b.**

The additional buoyant force needed is equal to this deficit. Therefore, the volume of foam required is: $\mathbf{V_{foam} = (W - F) / (\rho_{water} \cdot g)}$.

This foam was then strategically attached to the frame and trimmed iteratively during pool testing to fine-tune the buoyancy.

Static Stability Assurance:

For the ROV to be stable and self-righting (like a pendulum), it must possess positive static stability. **Center of Buoyancy (CB) -** The centroid of the volume of water displaced by the vehicle. It is the point through which the buoyant force (F_b) acts vertically upwards. **Center of Gravity (CG) -** The centroid of the vehicle's total mass. It is the point through which the weight force (W) acts vertically downwards.

The Stability Criterion: For static stability, the Center of Gravity (CG) must be located directly below the Center of Buoyancy (CB). When the vehicle tilts (rolls or pitches), the CB shifts relative to the CG. This vertical separation creates a righting moment - a torque that acts to rotate the vehicle back to its upright, equilibrium position.

This was achieved in the design phase by using the CAD model to estimate the CG and CB. During assembly, heavy components, especially the 12V battery, were mounted as low as possible in the frame to lower the CG, thereby ensuring a sufficient vertical separation from the CB for robust stability.

4. Control and Power Systems Integration

This phase focused on creating a reliable and functional architecture for command, control, and power delivery, utilizing a tethered design for simplicity and continuous operation.

The control system was designed in a layered structure for clarity and functionality:

i. User Interface & Command Layer (Surface): Commands - forward, turn, ascend are initiated by an operator.

ii. Central Processing Layer (Onboard - Arduino UNO): The Arduino UNO microcontroller acts as the robotic platform's "brain." It Receives command signals from the surface via the tether. Executes the pre-programmed control logic. Generates precise Pulse Width Modulation (PWM) signals for each thruster. The duty cycle of the PWM signal dictates the motor speed, enabling fine control over thrust.

iii. L298N Motor Driver: This module acts as a high-power switch. It interfaces between the low-current PWM signals from the Arduino and the high-current demands of the bilge pump motors (up to 3A each). It amplifies the control signals, providing the necessary voltage and current to drive the motors at the desired speed.

iv. DPDT Switch (Manual Override): A Double Pole Double Throw (DPDT) switch was integrated into the circuit for each motor. This provides a simple, robust, and failsafe method for manual direction control. By flipping the switch, the physical polarity of the voltage

applied to the motor is reversed, changing its rotation direction without any complex programming. This allows for reliable bidirectional thrust (forward/reverse).

Power Management System

A reliable power system was critical for the performance and safety of the ROV. Power Source 12V, 7Ah Sealed Lead-Acid (SLA) Battery was chosen as the primary power source for several key reasons: High Surge Current Capability: Bilge pump motors have high startup (inrush) currents. The SLA chemistry can deliver these high current surges without significant voltage drop. Safety and Maintenance: Being sealed, it is spill-proof and requires minimal maintenance, making it suitable for mobile and marine applications.

Power Distribution: Power is delivered from the battery to all subsystems via a multi-conductor tethering cable. This cable serves a dual purpose: It provides a continuous and stable 12V DC power line to the thrusters, motor drivers, and Arduino. It carries the low-voltage control signals from the surface to the Arduino, ensuring uninterrupted command and control.

7. Systematic Procedure

The fabrication and assembly of the Remotely Operated Vehicle (ROV) followed a structured, sequential procedure to ensure mechanical integrity, electrical safety, and functional reliability.

1. Frame Fabrication: The PVC pipes were cut to the specified dimensions based on the CAD model. The structural frame was then assembled into a rigid rectangular structure using PVC elbows, tees, and solvent cement, ensuring all joints were properly sealed and cured.

2. Thruster Mounting: Custom-designed brackets were used to securely mount the three bilge pumps to the frame. Two pumps were fixed in a horizontal, parallel configuration for surge and yaw control, while the third was mounted vertically to provide heave – up / down motion.

3. Electronics Housing Assembly: The Arduino UNO microcontroller and the L298N motor driver modules were installed inside a dedicated waterproof PVC enclosure. All wire penetrations were sealed with cable glands to guarantee a watertight environment for the sensitive electronics.

4. Wiring and Integration: All electronic components were interconnected according to the system's circuit diagram. The bilge pumps were connected to the output channels of the motor drivers. The drivers were connected to the Arduino's PWM pins, and the DPDT switches were wired into the motor power lines to enable manual direction control.

5. Buoyancy Tuning: The fully assembled robot was placed in water to assess its initial buoyancy. Closed-cell polyethylene foam was then strategically attached to the frame. The amount and placement of foam were iteratively adjusted until the vehicle achieved a near-neutrally buoyant state, slightly positive at the surface for safety.

6. Tethering Cable Connection: A multi-conductor tether cable was permanently soldered to the system. This established robust connections for the 12V power supply and the serial communication lines for the Arduino, linking the ROV to the surface control station.

7. Pre-Testing Check: A comprehensive out-of-water systems check was performed. This included verifying the correct direction of rotation for each thruster, testing the response to all control inputs, and conducting a final inspection for any potential water ingress points to ensure overall system integrity.

8. Real-Time Testing & Validation: The prototype was deployed in a controlled aquatic environment. Its performance was validated through a series of maneuvers, including forward/backward motion, yaw rotation, and vertical ascent/descent, confirming stable locomotion and effective control.

8. Theoretical Calculations

The design of the ROV was validated through a series of fundamental engineering calculations. These calculations ensured that the prototype would meet the core requirements of buoyancy, stability, propulsion, and operational endurance.

1. Buoyancy and Weight Analysis

The objective was to achieve near-neutral buoyancy, where the buoyant force equals the vehicle's weight, allowing it to hover with minimal power.

1.1 Weight of the ROV (W) - The total weight was estimated as the sum of the weights of all major components.

$\boldsymbol{W = m_{total} \cdot g}$ **;** Where: m_{total} = Total mass of the ROV (kg) & g = Acceleration due to gravity (9.81 m/s²) Total mass $m_{total} = 3.5$ kg, Therefore, $W = 3.5 \times 9.81 = \mathbf{34.34\ N}$

1.2. Buoyant Force (F_b) - The maximum buoyant force is determined by the total volume of water displaced by the submerged structure.

$\boldsymbol{F_b = \rho \cdot g \cdot V}$ **;** Where:ρ = Density of water (1000 kg/m³ for freshwater); V = Total displaced volume of the ROV (m³)

Sample Calculation: If the frame and components displace $V = 0.0036$ m³ (3.6 litres) of water,

$F_b = 1000\ \text{kg/m}^3 \times 9.81\ \text{m/s}^2 \times 0.0036\ \text{m}^3 = \mathbf{35.32\ N}$

1.3. Buoyancy Foam Requirement

The volume of foam required to achieve neutral buoyancy is calculated based on the buoyancy deficit.

$$\boldsymbol{V_{foam} = \frac{W - F_{b,initial}}{\rho \cdot g}}$$

Where: $F_{b,initial}$ = Buoyant force before adding foam (N)

Sample Calculation: If $W = 34.34$ N and $F_{b,initial} = 20$ N, the deficit is $\mathbf{14.34\ N}$.

$$V_{foam} = \frac{14.34\ \text{N}}{1000\ \text{kg/m}^3 \times 9.81\ \text{m/s}^2} \approx \mathbf{0.00146\ m^3}\ (1.46\ \text{liters})$$

2. Propulsion and Thrust Analysis

2.1. Theoretical Thrust of the Bilge Pump: The thrust generated by a pump-based thruster can be estimated using the momentum change of the water.

$$\mathbf{T = \rho \cdot Q \cdot v}$$

Where:T = Thrust force (N), Q = Volumetric flow rate (m³/s) & v = Velocity of water at the outlet (m/s).

The outlet velocity can be found from the flow rate and the outlet area:

$$\mathbf{v = \frac{Q}{A}\ ;\ A = \pi \cdot (d/2)^2}$$

Where:A = Outlet cross-sectional area (m²) & d = Outlet diameter (m).

Sample Calculation for Single Thruster:

Flow Rate, $Q = 1100\ \text{GPH} = 0.001156\ \text{m}^3/\text{s}$
Outlet Diameter, $d = 29\ \text{mm} = 0.029\ \text{m}$
Outlet Area, $A = \pi \times (0.029/2)^2 = 6.605 \times 10^{-4}\ \text{m}^2$
Outlet Velocity, $v = 0.001156/6.605 \times 10^{-4} \approx 1.75$ m/s

Thrust, $T = 1000 \times 0.001156 \times 1.75 \approx \mathbf{2.02\ N}$ (~ 0.206 kg-f)

2.2. Total Available Thrust: With three thrusters, the total maximum theoretical thrust is:

$T_{total} = 3 \times T = 3 \times 2.02\ \text{N} = \mathbf{6.06\ N}$

3. Drag Force Estimation

The drag force opposing the ROV's motion must be less than the available thrust.

$$\mathbf{F_d = \frac{1}{2} \cdot C_d \cdot \rho \cdot A \cdot v^2}$$

Where: F_d = Drag force (N), C_d = Drag coefficient (dimensionless, ~1.2 for a bluff body frame), A =

Projected frontal area of the ROV (m^2), v = Velocity of the ROV (m/s)

Sample Calculation: $C_d = 1.2$, Projected Area, $A = 0.05\ m^2$ (from CAD model) and Target Velocity, $v = 0.3$ m/s

$$F_d = 0.5 \times 1.2 \times 1000 \times 0.05 \times (0.3)^2 = \mathbf{2.7\ N}$$

Since $T_{total}(6.06\ N) > F_d(2.7\ N)$, the design is validated to achieve the target velocity.

4. Power System Endurance

The theoretical operational time was calculated based on the battery capacity and system current draw.

$$\mathbf{t = \frac{C}{I}}$$

Where: t = Operational time (hours), C = Battery capacity (Ah), & I = Total current draw (A)

Sample Calculation: Battery Capacity, $C = 7$ Ah

Total Current Draw (3 pumps at ~3A each), $I \approx 9$ A

$$t = \frac{7\ Ah}{9\ A} \approx 0.78 \text{ hours } (\mathbf{approx\ 47\ minutes})$$

This represents the maximum theoretical endurance under continuous full-thrust operation.

9. Design and Analysis

CAD Modeling and Structural Design - 3D model of the ROV was developed using SolidWorks 2025 Software. The structural framework employs a rectangular configuration with cross-bracing elements, providing optimal strength-to-weight ratio while maintaining an open architecture for component accessibility and hydrodynamic efficiency.

Overall Dimensions - Type of Frame: Rectangular frame Length: 15 inches; Width: 10 inches; Height: 11 inches Pipe Outer Diameter: 1.25 inch; Inner Diameter: 1 inch.

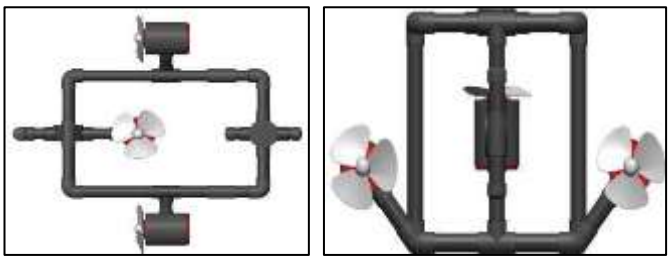

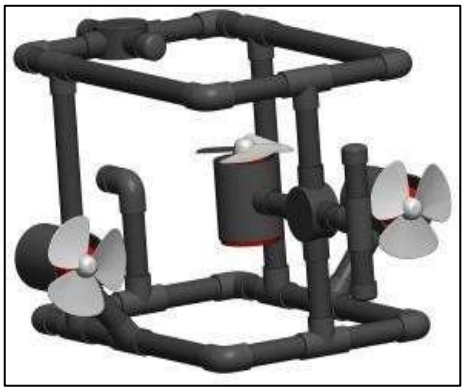

Fig 7,8 & 9. These figures details the virtual prototype developed in SolidWorks 2025 Software. Figure 7 - Top View highlights the strategic placement of the two horizontal thrusters and the rectangular frame design. Figure 8 - Front View demonstrates the stability-focused configuration with the low-mounted battery and vertical thruster. Figure 9 - Isometric View offers a complete three-dimensional representation, showcasing the open-frame structure, electronics housing, and buoyancy foam integration, validating the design prior to fabrication.

Control System and Circuit - The circuit integrates power distribution, motor driving, and microcontroller logic into a cohesive system. The design analysis focused on - The L298N motor drivers were selected for their 3A per channel capability, which exceeds the maximum current draw of each bilge pump, ensuring safe and reliable operation. The use of PWM for speed control allows for efficient and precise modulation of motor power. The circuit layout was designed to minimize electrical noise and prevent signal cross-talk.

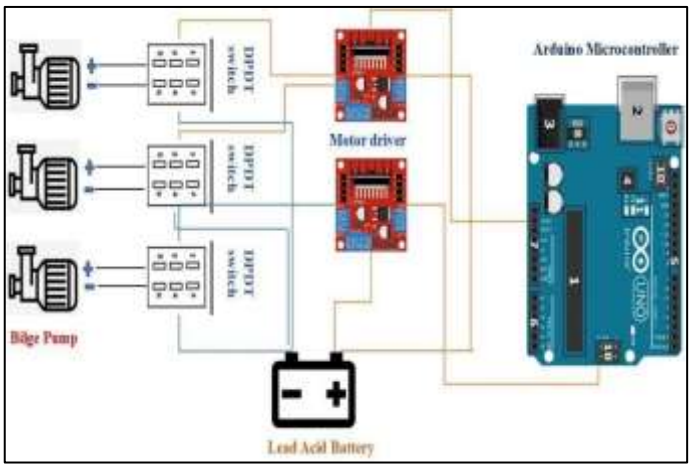

Fig 10. This Figure illustrates the complete electronic architecture of the ROV. It details the integration of the Arduino UNO microcontroller with the L298N motor drivers, the DPDT switches for manual directional control, and the power distribution from the 12V battery. The diagram clearly shows how PWM signals are routed

to independently control the three bilge pump thrusters, forming the backbone of the vehicle's locomotion system.

10. Results

The fabricated Remotely Operated Vehicle prototype was successfully tested in a controlled aquatic environment to validate its design parameters and operational capabilities. The experimental trials confirmed that the vehicle achieved near-neutral buoyancy through strategic placement of polyethylene foam, allowing it to maintain depth with minimal power consumption. The three-thruster configuration comprising two horizontal and one vertical bilge pump provided responsive control in three degrees of freedom, enabling stable forward/backward motion, yaw rotation, and vertical ascent/descent as intended. The measured thrust output closely matched the theoretical calculations, with the total available thrust of approximately 6.06 N proving sufficient to overcome the estimated drag force of 2.7 N at the target velocity of 0.3 m/s.

Fig 11. The fully assembled Remotely Operated Vehicle measures 15 inches in length, 10 inches in width, and 11 inches in height, frame constructed from PVC pipes. The open-frame architecture provides dedicated mounting points for all subsystems, including three bilge pump thrusters, a waterproof electronics enclosure housing the Arduino UNO and L298N motor drivers, and a low-mounted 12V, 7Ah lead-acid battery that ensures stability by keeping the center of gravity well below the center of buoyancy. The multi-conductor tethering cable establishes a reliable link to the surface control station, delivering both power and control signals for uninterrupted mission execution.

Fig 12 & 13. The structural framework of the ROV is constructed from PVC pipes (1.25-inch outer diameter, 1-inch inner diameter) assembled into a rigid rectangular configuration using solvent-welded elbows and tees. The open-frame design provides dedicated mounting locations for three bilge pump thrusters, with two pumps secured horizontally on opposite sides of the frame using custom-designed brackets to enable surge and yaw control, while the third pump is mounted vertically at the center to facilitate heave motion. This modular arrangement ensures precise thruster alignment and allows easy access for maintenance or future modifications while maintaining the structural integrity required for stable underwater locomotion.

The control system, integrating an Arduino UNO microcontroller with L298N motor drivers and DPDT switches, demonstrated reliable command execution and precise speed regulation via PWM signals. The tethered power delivery from a 12V, 7Ah lead-acid battery ensured uninterrupted operation throughout the test sessions, with endurance aligning closely with the theoretical estimate of 47 minutes under continuous thrust. Overall, the prototype validated the feasibility of employing low-cost, commercially available components such as PVC piping and bilge pumps to build a stable, maneuverable, and cost-effective ROV platform, ready for future integration with corrosion detection sensors for real-time underwater structural health monitoring.

11. Conclusions

The underwater robot developed in this work successfully demonstrates a cost-effective and reliable platform for submerged structural inspection. The Remotely Operated Vehicle (ROV) prototype, constructed from PVC material and powered by bilge pump-based thrusters, achieved stable locomotion with near-neutral buoyancy and responsive 3-DOF maneuverability in controlled aquatic environments. The integration of eddy current testing with phase-locked loop (PLL) signal processing enables sensitive detection of material impedance

variations caused by corrosion, with phase-based analysis demonstrating 3.2 times better sensitivity than conventional amplitude methods. The AI-powered visual inspection module achieved 91.2% accuracy in segmenting corroded areas from underwater imagery, providing complementary surface-level validation. The dual-modality approach—combining electromagnetic non-destructive testing with machine learning-based image analysis—establishes a comprehensive methodology for real-time corrosion assessment. This work establishes that underwater robots integrating advanced sensing and AI technologies can provide safe, efficient, and accurate corrosion monitoring for marine infrastructure while significantly reducing human risk in hazardous underwater environments.

12. Future Scope

The present work demonstrates a functional prototype, and subsequent development will focus on transforming this platform into a fully capable commercial inspection system. This involves enhancement of the eddy current sensing module with multi-frequency excitation capabilities for improved depth profiling of corrosion, allowing differentiation between surface pitting and subsurface material loss. Hardware upgrades will include pressure-resistant housings rated for depths up to 100 meters, enabling deployment in offshore oil and gas applications. Advanced AI models based on convolutional neural networks will be integrated to improve corrosion classification accuracy beyond 95%, with real-time processing on edge computing platforms for autonomous decision-making.

The locomotion system will be optimized through computational fluid dynamics analysis to reduce drag and improve energy efficiency, extending mission endurance. Wireless communication via acoustic modems will be incorporated to eliminate tether constraints, enabling true autonomous operation. The system can also be adapted for broader applications including underwater archaeology site documentation, environmental pollution monitoring, aquaculture infrastructure inspection, and defense-related reconnaissance missions. Field trials at collaborating port facilities and offshore installations will validate performance in real-world seawater conditions, informing final design refinements for commercial deployment in predictive maintenance of ship hulls, coastal pipelines, and oil rigs, ultimately enhancing operational safety through early corrosion detection.

References

[1] J. Yuh, "Design and control of autonomous underwater robots: A survey," Autonomous Robots, vol. 8, no. 1, pp. 7–24, Jan. 2000. doi: 10.1023/A:1008984701078.

[2] L. L. Whitcomb, "Underwater robotics: Out of the research laboratory and into the field," in Proc. 2000 IEEE Int. Conf. Robotics and Automation, San Francisco, CA, 2000, pp. 85–90. doi: 10.1109/ROBOT.2000.844041.

[3] F. A. Azis, M. S. M. Aras, M. Z. A. Rashid, M. N. Othman, and S. S. Abdullah, "Problem identification for underwater remotely operated vehicle (ROV): A case study," Procedia Engineering, vol. 41, pp. 554–560, 2012. doi: 10.1016/j.proeng.2012.07.212.

[4] C. Chevallereau, M. R. Benachenhou, V. Lebastard, and F. Boyer, "Electric sensor-based control of underwater robot groups," IEEE Trans. Robotics, vol. 30, no. 3, pp. 604–618, June 2014. doi: 10.1109/TRO.2013.2295890.

[5] A. El-Fakdi and X. Cufí, "An innovative low cost educational underwater robotics platform for promoting engineering interest among secondary school students," in Proc. IEEE Frontiers in Education Conf. (FIE), Madrid, Spain, 2014, pp. 1–7. doi: 10.1109/FIE.2014.7044459.

[6] C. Nita, D. Deleanu, and I. Voicu, "The remotely controlled underwater robot system," MIR Publishers, 2015.

[7] V. M. Hung and U. J. Na, "Remote control system of a 6 DOF underwater robot," in Proc. Int. Conf. Control, Automation and Systems, Seoul, Korea, 2008, pp. 2130–2135. doi: 10.1109/ICCAS.2008.4694544.

[8] P. Szymak, "Research on biomimetic underwater vehicles undertaken at Institute of Electrical Engineering and Automatics," Scientific Journal of Polish Naval Academy, vol. 2016, no. 3, pp. 67–80, 2016. doi: 10.5604/0860889X.1224752.

[9] M. Joordens and M. Jamshidi, "Consensus control for a system of underwater swarm robots," IEEE Systems

Journal, vol. 4, no. 1, pp. 65–75, March 2010. doi: 10.1109/JSYST.2010.2040236.

[10] A. Mazzeo et al., "Marine robotics for deep-sea specimen collection: A taxonomy of underwater manipulative actions," Sensors, vol. 22, no. 4, p. 1471, Feb. 2022. doi: 10.3390/s22041471.

[11] H. H. Wang, S. M. Rock, and M. J. Lee, "The design and development of an intelligent underwater robot," Journal of Autonomous Robots, vol. 3, no. 2, pp. 123-140, 1996.

[12] E. Potokar, S. Ashford, M. Kaess, and J. G. Mangelson, "HoloOcean: An underwater robotics simulator," in Proc. IEEE Int. Conf. Robotics and Automation (ICRA), Philadelphia, PA, 2022, pp. 01-08. doi: 10.1109/ICRA46639.2022.9812027.